HW1

June 16, 2019

1 Q1

1. Advantage:

Cameras and inertial measurement unit (IMU) sensor are complimentary with one another in a way which would be able to compensate for the errors made by each of them via the redundant information they provided.

IMU 与视觉定位方案优势与劣势对比：

方案	IMU	视觉
优势	快速响应 不受成像质量影响 角速度普遍比较准确 可估计绝对尺度	不产生漂移 直接测量旋转与平移
劣势	存在零偏 低精度 IMU 积分位姿发散 高精度价格昂贵	受图像遮挡、运动物体干扰 单目视觉无法测量尺度 单目纯旋转运动无法估计 快速运动时易丢失

(a)

整体上，视觉和 IMU 定位方案存在一定互补性质：

- IMU 适合计算短时间、快速的运动；
- 视觉适合计算长时间、慢速的运动。

同时，可利用视觉定位信息来估计 IMU 的零偏，减少 IMU 由零偏导致的发散和累积误差；反之，IMU 可以为视觉提供快速运动时的定位。

(b)

Figure 1: Advantage vs Disadvantage

2. Approaches (or techniques):

Filtering-based approaches: (MSCKF)

The EKF framework generally consists of a prediction and an updating step. The inertial sensors are able to provide acceleration and rotation velocity measurements in three axes, which serve as the data-driven dynamic model or prior distribution for a 3D rigid body motion or prior distribution for a 3D rigid body motion and make the motion prediction in the prediction step. Cameras provide the angular and ranging measurements between features and the mobile plat-from, which serve as the measurement model and update the prediction results in updating step.

Optimization-based approaches. (VINS)

These approaches mainly rely on the techniques of image processing for feature extraction and optimization for image alignment, while inertial measurement is treated as prior or regularization terms. The two stages in this kind of approach: mapping and tracking.

Industrial Example: Some AR application.

3. Academic Progress:

Semantic localization and mapping [1]:

A few recent research efforts have attempted to endow VINS with semantic understanding of environments, which is only sparsely explored but holds great potentials.

Extensions to different aiding sensors [1]:

While optical cameras are seen an ideal aiding source for INS in many applications, other aiding sensors may more proper for some environments and motions, for example, acoustic sonars may be instead used in underwater; low-cost light-weight LiDARs may work better in environments, e.g., with poor lighting conditions; and event cameras may better capture dynamic motions. Along this direction, we should investigate in-depth VINS extensions of using different aiding sources for applications at hand.

Reference: https://arxiv.org/pdf/1906.02650.pdf

2 Q2

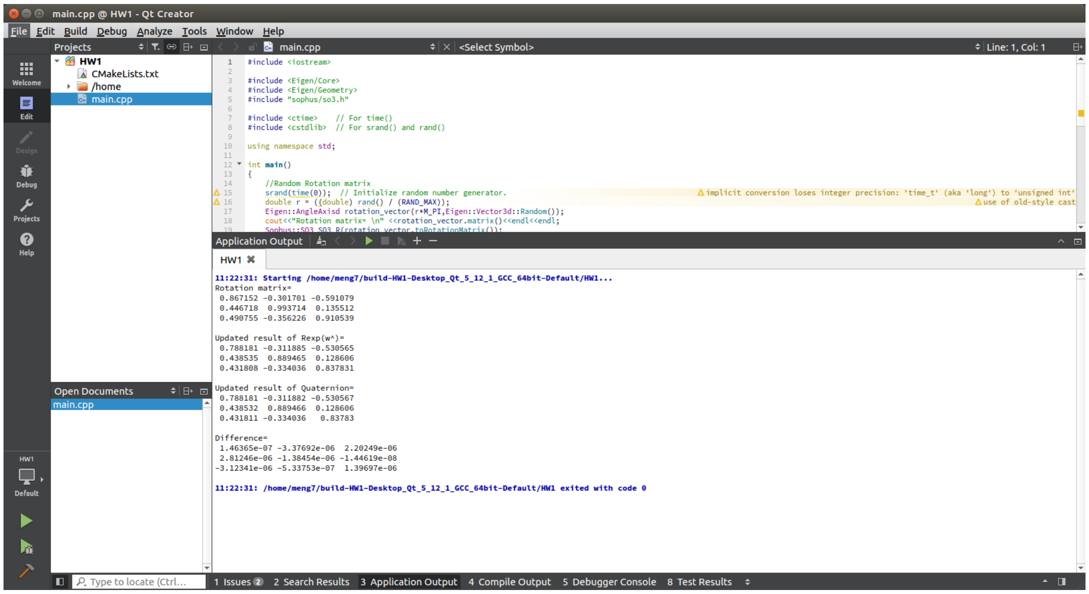

Figure 2: Result

3 Q3

1. Assume the perturbation ΔR and the corresponding lie algebra ϕ,

$$\begin{aligned}
\frac{d(\mathbf{R}^{-1}\mathbf{p})}{d\mathbf{R}} &= \lim_{\phi\to 0} \frac{(\mathbf{R}\exp((\phi^\wedge))^{-1}\mathbf{p} - \mathbf{R}^{-1}\mathbf{p}}{\phi} \\
&= \lim_{\phi\to 0} \frac{\exp(-\phi^\wedge)\mathbf{R}^{-1}\mathbf{p} - \mathbf{R}^{-1}\mathbf{p}}{\phi} \approx \lim_{\phi\to 0} \frac{(\mathbf{I} - \phi^\wedge)\mathbf{R}^{-1}\mathbf{p} - \mathbf{R}^{-1}\mathbf{p}}{\phi} \\
&= \lim_{\phi\to 0} \frac{-\phi^\wedge(\mathbf{R}^{-1}\mathbf{p})}{\phi} \\
&= \lim_{\phi\to 0} \frac{(\mathbf{R}^{-1}\mathbf{p})^\wedge\phi}{\phi} \\
&= (\mathbf{R}^{-1}\mathbf{p})^\wedge
\end{aligned} \tag{1}$$

2.

$$\begin{aligned}
\frac{\mathrm{d}\ln\left(\mathbf{R}_1\mathbf{R}_2^{-1}\right)^\vee}{\mathrm{d}\mathbf{R}_2} &= \lim_{\phi\to 0} \frac{(\mathbf{R}_1(\mathbf{R}_2\exp(\phi^\wedge))^{-1})^\vee - \ln(\mathbf{R}_1\mathbf{R}_2^{-1})^\vee}{\phi} \\
&= \lim_{\phi\to 0} \frac{\ln(\mathbf{R}_1\exp(-\phi)^\wedge\mathbf{R}_2^{-1})^\vee - \ln\left(\mathbf{R}_1\mathbf{R}_2^{-1}\right)^\vee}{\phi}
\end{aligned} \tag{2}$$

According to the principal of adjoint,

$$\begin{aligned}\mathbf{R_1}\exp\left(-\phi^\wedge\right)\mathbf{R_2}^{-1} =&\mathbf{R_1}\mathbf{R_2}^{-1}\mathbf{R_2}\exp\left(-\phi^\wedge\right)\mathbf{R_2}^T \\ =&\mathbf{R_1}\mathbf{R_2}^{-1}\exp\left((-\mathbf{R_2}\phi)^\wedge\right)\end{aligned} \tag{3}$$

We also have,

$$\ln\left(\mathbf{R}\exp\left(\boldsymbol{\phi}^\wedge\right)\right)^\vee = \ln(\mathbf{R})^\vee + \mathbf{J}_r^{-1}\boldsymbol{\phi} \tag{4}$$

As a result,

$$\begin{aligned}\frac{\mathrm{d}\ln\left(\mathbf{R}_1\mathbf{R}_2^{-1}\right)^\vee}{\mathrm{d}\mathbf{R}_2} &= \lim_{\phi\to 0}\frac{\ln(\mathbf{R_1}\mathbf{R_2}^{-1}\exp\left((-\mathbf{R_2}\phi)^\wedge\right))^\vee - \ln\left(\mathbf{R}_1\mathbf{R}_2^{-1}\right)^\vee}{\phi} \\ &= \lim_{\phi\to 0}\frac{\ln(\mathbf{R}_1\mathbf{R}_2^{-1})^\vee + \mathbf{J}_r^{-1}(-\mathbf{R_2}\phi) - \ln\left(\mathbf{R}_1\mathbf{R}_2^{-1}\right)^\vee}{\phi} \\ &= -\mathbf{J}_r^{-1}(\ln\left(\mathbf{R_1}\mathbf{R_2}^{-1}\right)^\vee)(\mathbf{R_2})\end{aligned} \tag{5}$$

References

[1] G. Huang, "Visual-inertial navigation: A concise review," *arXiv preprint arXiv:1906.02650*, 2019.